



สมบัติเทอร์โมอิเล็กทริกและสมบัติแม่เหล็กของ $\text{La}_{0.7}(\text{Sr}_{1-x}\text{Ca}_x)_{0.3}\text{MnO}_3$ ที่สังเคราะห์ด้วยวิธีการสลายตัวทางความร้อนโดยใช้น้ำ

Thermoelectric and Magnetic Properties of $\text{La}_{0.7}(\text{Sr}_{1-x}\text{Ca}_x)_{0.3}\text{MnO}_3$ Synthesized by Thermal Hydro-Decomposition Method

สุปรีดี พินิจสุนทร (Supree Pinitsoontorn)^{1*}
 มัตติกา พ่วง (Muttika Phewbang)¹

¹ Department of Physics, Faculty of Science, Khon Kaen University, Khon Kaen, 40002, Thailand

* E-mail: psupree@kku.ac.th; Tel. 080-4012471

บทคัดย่อ

วัสดุ $\text{La}_{0.7}(\text{Sr}_{1-x}\text{Ca}_x)_{0.3}\text{MnO}_3$ ที่ $x = 0.0, 0.2, 0.4, 0.6, 0.8$ และ 1.0 ถูกสังเคราะห์ขึ้นด้วยวิธีการสลายตัวทางความร้อนโดยใช้น้ำ ใช้สารตั้งต้นประเภทโลหะอะซิเตท กับน้ำปราศจากไออกอน ทำการศึกษาลักษณะทางกายภาพของสารที่สังเคราะห์ขึ้นโดยเทคนิคเทอร์มอกราเวมทริก/ดิฟเฟอเรนเชียลเทอร์มัลอะโนดิชิก (TG/DTA), เทคนิคการเลือบabenของรังสีเอกซ์ (XRD), การวิเคราะห์หานปริมาณธาตุด้วยการวัดระดับการกระจายพลังงานของรังสีเอกซ์ (EDX) และการถ่ายภาพด้วยกล้องจุลทรรศน์อิเล็กตรอนแบบส่องการดู (SEM) ผลการวิเคราะห์พบว่า สามารถสังเคราะห์เฟสเดียวของพหุผลึก $\text{La}_{0.7}(\text{Sr}_{1-x}\text{Ca}_x)_{0.3}\text{MnO}_3$ โดยการเผาแคลไชน์ที่อุณหภูมิ $800\text{ }^\circ\text{C}$ เป็นเวลา 4 h แต่ยังมีเฟสเจือปนหลงเหลืออยู่ หลังจากนั้นอัดขึ้นรูปด้วยวิธีอัดเกนเดียว ด้วยความดัน 50 MPa และเผาเผนกีที่อุณหภูมิ $1,200\text{ }^\circ\text{C}$ เป็นเวลา 6 h ไม่เจือปนหายไป ผลการศึกษาสมบัติทางเทอร์โมอิเล็กทริกที่อุณหภูมิห้องพบว่า ที่ค่า $x = 1.0$ วัสดุมีค่าส่วนตัวทางไฟฟ้าและสัมประสิทธิ์ซึ่งคุ้งสุด เท่ากับ $2.2\text{ }\Omega\text{cm}$ และ $91\text{ }\mu\text{VK}^{-1}$ ตามลำดับ ส่วนผลการศึกษาสมบัติทางแม่เหล็กพบว่า ที่ค่า $x = 0$ วัสดุมีค่าแม่กนีไดเซชันสูงสุดเท่ากับ 20 emu/g

Abstract

$\text{La}_{0.7}(\text{Sr}_{1-x}\text{Ca}_x)_{0.3}\text{MnO}_3$ powders for $x = 0.0, 0.2, 0.4, 0.6, 0.8$ and 1.0 were synthesized by a thermal hydro-decomposition method using metal acetate salts and de-ionized water as starting materials. The physical properties of the samples were characterized by thermogravimetric/ differential thermal analysis (TG/DTA), x-ray diffraction (XRD), energy dispersive x-ray analysis (EDX) and scanning electron microscopy (SEM). The single phase of $\text{La}_{0.7}(\text{Sr}_{1-x}\text{Ca}_x)_{0.3}\text{MnO}_3$ compound was obtained at the calcined temperature of $800\text{ }^\circ\text{C}$ for 4 h , but some second phases were still observed. The polycrystalline bulk samples were compacted by a uniaxial pressure of 50 MPa and then sintered at $1,200\text{ }^\circ\text{C}$ for 6 h . The second phases were disappeared. The thermoelectric properties of the sintered samples were investigated at room temperature and found that at $x = 1.0$, the electrical resistivity and the Seebeck coefficient were $2.2\text{ }\Omega\text{cm}$ and $91\text{ }\mu\text{VK}^{-1}$, respectively. The magnetic properties study showed that at $x = 0$ the maximum magnetization was found to be 20 emu/g .

คำสำคัญ: $\text{La}_{0.7}(\text{Sr}_{1-x}\text{Ca}_x)_{0.3}\text{MnO}_3$, การสลายตัวทางความร้อน, สมบัติเทอร์โมอิเล็กทริก, สมบัติแม่เหล็ก

Keywords: $\text{La}_{0.7}(\text{Sr}_{1-x}\text{Ca}_x)_{0.3}\text{MnO}_3$, Thermal decomposition, Thermoelectric properties, Magnetic properties

Introduction

Thermoelectric generators can convert waste heat, produced by many sources such as automotive exhaust, solar radiation, and industrial processes, electricity. Conversely, thermoelectric coolers can be used to make refrigerators and other cooling systems. This energy conversion process produces no waste substance and is environmentally friendly. Generally, the performance of a thermoelectric material is evaluated in terms of the dimensionless figure of merit, $ZT = S^2 T / rk$ where, S , r , k , and T are Seebeck coefficient, electrical resistivity, thermal conductivity and absolute temperature, respectively. As a result, a good thermoelectric material should simultaneously exhibit small r and k and large S . For practical application, ZT should be more than 1.0.

Thermoelectric materials are conventionally made of metallic compounds such as Bi_2Ti_3 or PbTe (1) due to their excellent efficiency at room temperature. However, such compounds are not reliable and chemically unstable at high temperature. Oxides materials in general are chemically stable at high temperature and, thus, can be used at the temperature of several hundred °C (2). Shikano and Funahashi reported that the single crystal $\text{Ca}_3\text{Co}_4\text{O}_9$ have a high thermoelectric figure merit ZT nearly 0.87 at 700 °C, which indicates that oxide materials have a high potential for practical application in thermoelectric power generation at high temperature (3). Apart from the group of $\text{Ca}_3\text{Co}_4\text{O}_9$, other oxide materials have been studied for thermoelectric application such as ZnO , SrTiO_3 or compounds of manganite (MnO_3) (4).

The perovskite manganite based materials, $\text{Ln}_{1-x}\text{D}_x\text{MnO}_3$ (where Ln is La, Pr, Nd, Eu, Y, etc. and D is Ca, Sr, Pb, Ba, etc.) have received much intention from several research groups due to its unique properties and potential for future application. In particular, $\text{La}_{1-x}\text{Sr}_x\text{MnO}_3$ compounds, has been intensively studied for their interesting magnetic properties (5, 6). Moreover, some

research groups have studied the thermoelectric properties of $\text{La}_{1-x}\text{Ca}_x\text{MnO}_3$ (7) and tried to improve such properties by doping some elements such as Te (8), or Y (9) at the Ca site. In this paper, we synthesized $\text{La}_{0.7}\text{Sr}_{0.3}\text{MnO}_3$ nanopowders using the simple thermal hydro-decomposition method (10), and then gradually substitute Ca for Sr. We measured the substitution effect on magnetic and thermoelectric properties.

Experimental Method

Nanocrystalline powders of $\text{La}_{0.7}(\text{Sr}_{1-x}\text{Ca}_x)_{0.3}\text{MnO}_3$ ($x = 0.0, 0.2, 0.4, 0.6, 0.8$ and 1.0) were synthesized using a thermal hydro-decomposition method. The acetate salt of La, Sr, Ca and Mn in the stoichiometric ratio was dissolved in DI water in the ratio of 1 g of the starting materials / 5 ml of water. The mixture was thoroughly stirred until the completely mixed solution was formed. Then, the solution was heated in a furnace to 800 °C with the rate of 5 °C/minute and annealed for 4 h. The black powders were obtained. Phase formation analysis was carried out using thermogravimetric/differential thermal analysis (TG/DTA). The phase identification of the obtained samples was verified by x-ray diffraction (XRD) at room temperature. Energy Dispersive x-ray spectroscopy (EDX) was a microanalytical technique used to obtain information about elemental composition of the sample. The morphology of the samples was observed by scanning electron microscopy (SEM). For magnetic properties measurement, the powders were investigated using a vibrating sample magnetometer (VSM) at room temperature. To measure the thermoelectric properties, the bulk samples were prepared. The powders were regrounded and uniaxially pressed at 50 MPa to form pellets with a diameter of 16 mm which were sintered at 1200 °C for 6 hours in air. The seebeck coefficient was measured by plotting the voltage difference against the temperature gradient. The resistivity was measured using

a standard four probe technique using the Van der Pauw method.

Results and Discussion

Fig. 1 shows the DTA and the TG curves of the dried solution of $\text{La}_{0.7}(\text{Sr}_{1-x}\text{Ca}_x)_{0.3}\text{MnO}_3$ at the temperature range of 100 – 1000 °C. The TG/DTA analysis was chosen for a comparison between $x = 0$ (no Ca substitution), and $x = 0.8$. It can be seen that both curves in Fig. 1 (a) and (b) are not significantly different. A few exothermic peaks of the sample occurring during 130-400 °C corresponded to the decomposition of organic substance in the mixture. From 200- 800°C, significant weight loss of nearly 20% was attributed to the formation of $\text{La}_{0.7}(\text{Sr}_{1-x}\text{Ca}_x)_{0.3}\text{MnO}_3$ from the free metallic ions. The compound was believed to be nucleated at the temperature of 600-700 °C, and completed at temperature over 850 °C as one can see no change in weight loss above over 850 °C

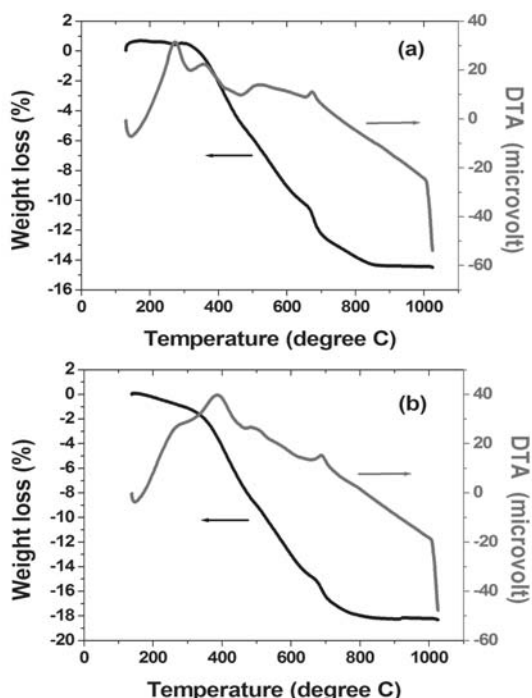


Fig.1 TG/DTA curves of the dried solution of $\text{La}_{0.7}(\text{Sr}_{1-x}\text{Ca}_x)_{0.3}\text{MnO}_3$ for (a) $x = 0$ and (b) $x = 0.8$

The XRD patterns of the $\text{La}_{0.7}(\text{Sr}_{1-x}\text{Ca}_x)_{0.3}\text{MnO}_3$ powders for all x values are shown in Fig. 2 (a). All diffraction peaks are identical with the JCPDS card No. 51-0409 for the perovskite structure of $\text{La}_{0.7}\text{Sr}_{0.3}\text{MnO}_3$, and can be matched with previous reports (5, 6). This means that the thermal hydro-decomposition method was successfully exploited in synthesizing the $\text{La}_{0.7}(\text{Sr}_{1-x}\text{Ca}_x)_{0.3}\text{MnO}_3$ compounds. and Ca atoms were successfully substituted at the Sr site. However, the peak at $2\theta \sim 65^\circ$, corresponding to a second phase, can be seen for $x = 0.2$ and 1.0. In Fig. 2 (b), the XRD patterns of the sintered $\text{La}_{0.7}(\text{Sr}_{1-x}\text{Ca}_x)_{0.3}\text{MnO}_3$ ceramics for different x values are presented. It can be obviously seen that after sintering the XRD peaks are sharper and the full width at half maximum is much narrower. This can be implied that the crystallinity of $\text{La}_{0.7}(\text{Sr}_{1-x}\text{Ca}_x)_{0.3}\text{MnO}_3$ is fully completed. Furthermore, the second phase peak found in the calcined samples is

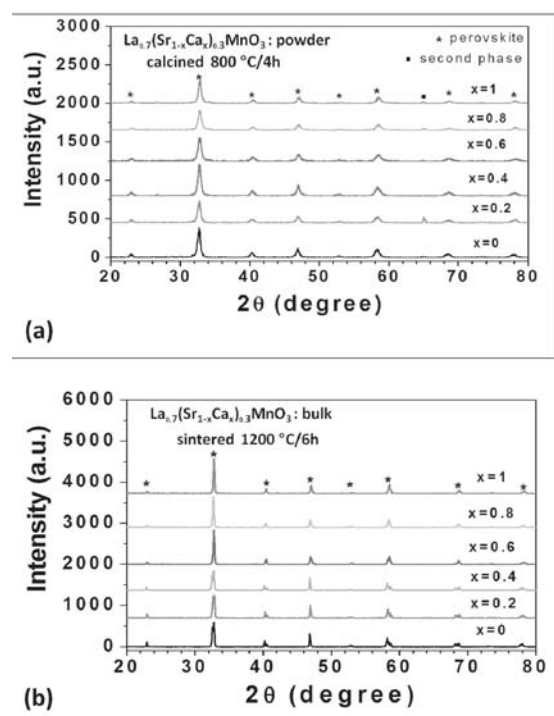


Fig.2 XRD patterns of $\text{La}_{0.7}(\text{Sr}_{1-x}\text{Ca}_x)_{0.3}\text{MnO}_3$ for (a) the calcined powder for different x values and (b) the sintered ceramics for different x values

completely disappeared after sintering. This shows an increase in purity of the synthesized materials. Another obvious feature that can be seen from Fig. 2 (b) is the split of the XRD peaks, particularly at high angle, for $x = 0, 0.2, 0.4$, and very few for $x = 0.6$. This is the characteristic of the rhombohedral structure from the distorted perovskite structure. The peak splitting was not found for the case of $x = 0.8$ and 1.0 , indicating the perovskite cubic structure. For Fig. 2 (a), the peak splitting cannot be seen because the particle size is so small that causes peak broadening and overlapping.

The morphology of the calcined powders was studied by the SEM micrographs as shown in Fig. 3. It can be seen that the shape of all powders was spherical and the powders were clustered to form larger groups of particles. The average size of the powders, calculated by counting the size of 200 particles for each sample, was found to be in the range of 100-200 nm, with the maximum standard deviation of ± 60 nm. Fig. 4 shows the SEM micrographs of the sample after the sintering process. It can be obviously seen that the interconnecting grains were formed after sintering, with significant reduction of porosity. However, the grain size of the bulk samples in the order $1.0 \pm 0.3 \mu\text{m}$

for all samples appeared to be much larger than the synthesized powders. This is possibly due to the high sintering temperature and long sintering time. In addition, elemental analysis was obtained from EDX and showed that the specimen consisted of La, Sr, Ca, Mn and O. Quantitative analysis showed that the atomic ratios of La: Sr: Ca: Mn were close to the nominal composition but the oxygen composition varies slightly from one sample to the others due to the limit of the EDX technique.

Fig. 5 shows the electrical resistivity (r) and the Seebeck coefficient (S) of the sintered ceramics $\text{La}_{0.7}(\text{Sr}_{1-x}\text{Ca}_x)_{0.3}\text{MnO}_3$ for different x values at room temperature. The sign of S was positive over the entire range of x values, indicating p-type conduction. It can be seen that both the resistivity and the Seebeck coefficient increased with the higher content of Ca. The lowest r and S were found to be approximately $0.25 \Omega\text{cm}$ and $10 \mu\text{VK}^{-1}$, respectively, for $x = 0$. The largest r and S were found to be approximately $2.2 \Omega\text{cm}$ and $91 \mu\text{VK}^{-1}$, respectively, for $x = 1$, which was equivalent to the power factor (S^2/r) of $0.38 \mu\text{Wm}^{-1}\text{K}^{-2}$ at room temperature. The power factor observed in our study was higher than the previous study on $\text{La}_{0.7}\text{Ca}_{0.3}\text{MnO}_3$ (7).

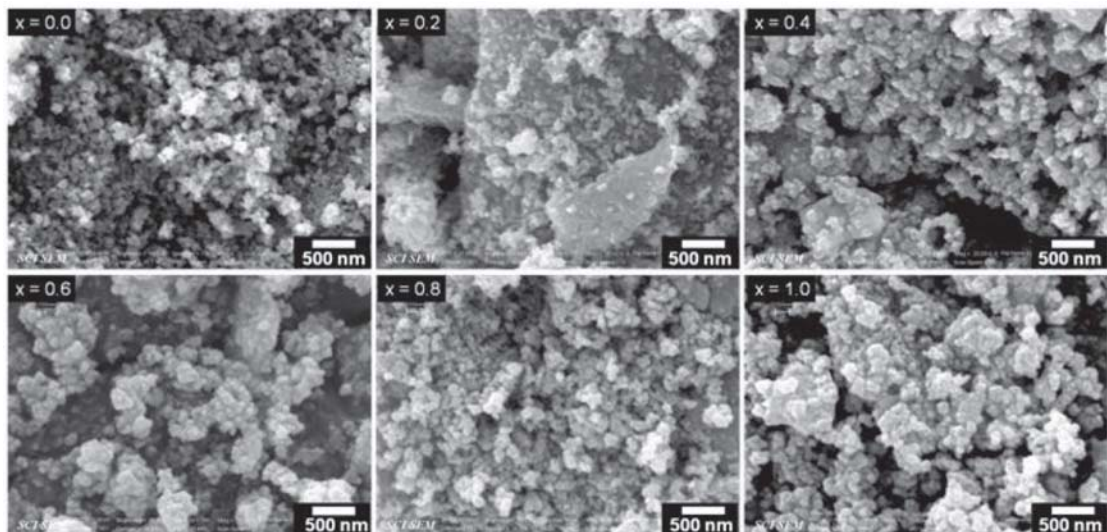


Fig. 3 SEM micrographs of the calcined powder $\text{La}_{0.7}(\text{Sr}_{1-x}\text{Ca}_x)_{0.3}\text{MnO}_3$ for different x values

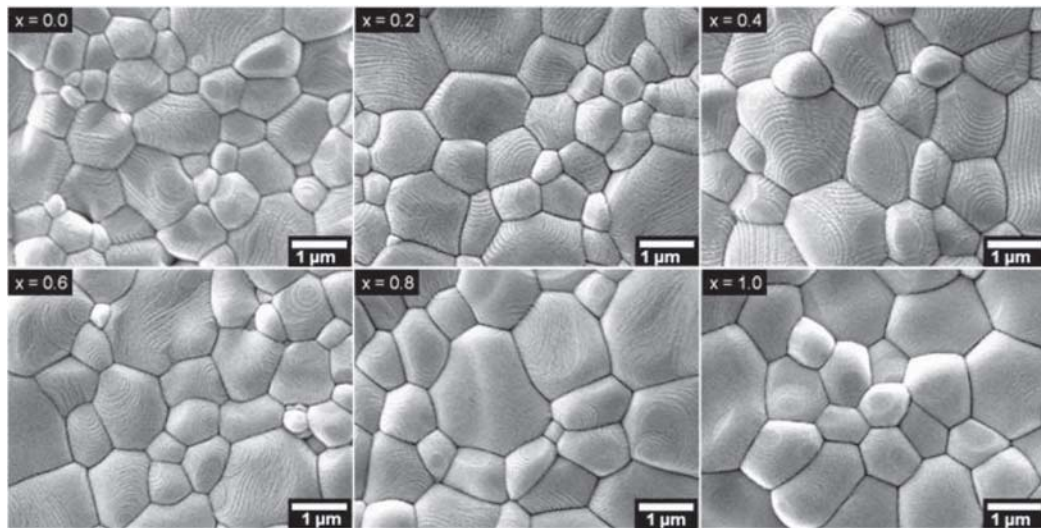


Fig. 4 SEM micrographs of the sintered ceramics $\text{La}_{0.7}(\text{Sr}_{1-x}\text{Ca}_x)_{0.3}\text{MnO}_3$ for different x values

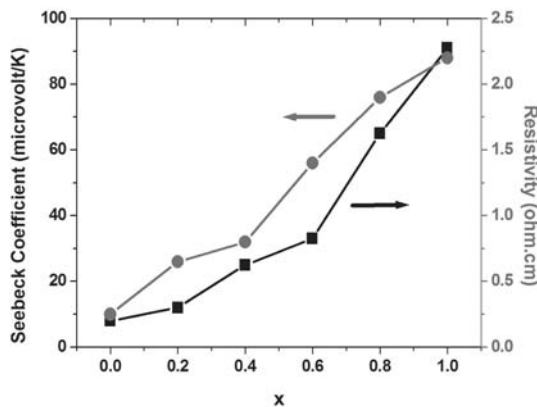


Fig. 5 Room temperature Seebeck coefficient and electrical resistivity of the sintered ceramics $\text{La}_{0.7}(\text{Sr}_{1-x}\text{Ca}_x)_{0.3}\text{MnO}_3$ for different x values

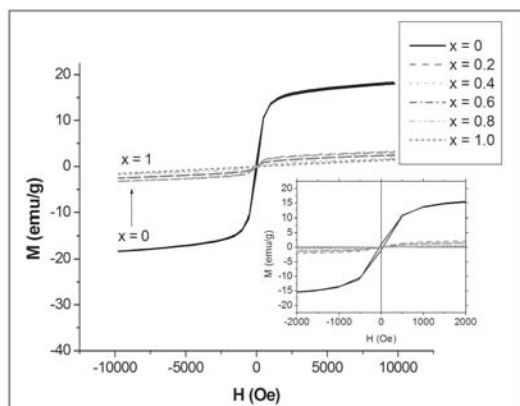


Fig. 6 Room temperature magnetic properties of the $\text{La}_{0.7}(\text{Sr}_{1-x}\text{Ca}_x)_{0.3}\text{MnO}_3$ powders for different x values

The magnetic properties of the $\text{La}_{0.7}(\text{Sr}_{1-x}\text{Ca}_x)_{0.3}\text{MnO}_3$ powders measured by using VSM are shown in Fig. 5. It can be clearly seen that without Ca substitution, $\text{La}_{0.7}\text{Sr}_{0.3}\text{MnO}_3$ powders behave as a strong ferromagnetic material. As the Ca content was added, the magnetization was significantly reduced. Even for a slight Ca content of $x = 0.2$, the magnetization quickly dropped from nearly 20 emu/g to below 3 emu/g. This is quite a surprising result because Sr and Ca ions have the same ionic charge of +2. The Ca partial substitution should neither change the overall or local electrical potential nor the electronic configuration which can alter the magnetic moments. However, the ionic radii of Sr and Ca are different, and this may be the primary effect that could lower the magnetization even for little Ca substitution. It is well known that $\text{La}_{0.7}\text{Sr}_{0.3}\text{MnO}_3$ exhibits large magnetic moment (5) and the magnetic moment alignment is crucially controlled by the distance between neighbor atoms. Replacing Sr atoms with different size Ca atoms would cause the strain and distortion which consequently change the neighbor atomic distance, and hence the magnetic properties. The underlying physics of the change in magnetic properties may be attributed to the change in spin-orbit coupling due to a decrease in unit cell size.

Conclusions

Homogeneous and single phase $\text{La}_{0.7}(\text{Sr}_{1-x}\text{Ca}_x)_{0.3}\text{MnO}_3$ compounds were successfully synthesized through the thermal hydro-decomposition method. The $\text{La}_{0.7}(\text{Sr}_{1-x}\text{Ca}_x)_{0.3}\text{MnO}_3$ powders were obtained by calcining the mixed solution at 800 °C for 4 h. The polycrystalline bulk samples were fabricated by a uniaxial pressing at 50 MPa and afterward sintered at 1200 °C for 6 h. Ca atoms successfully substituted for Sr without changing its crystal structure. Crystallite sizes were in the range of 100 nm while the sintered grain sizes were about 1.0 μm . The measured thermoelectric and magnetic properties were found to be sensitive to the elemental contents, with the highest thermoelectric power factor for $x = 1.0$ sample and the highest magnetization for $x = 0$ sample.

Acknowledgement

This project funding was supported by the Office of Research Administration under the New Researcher Development Program 2008, Khon Kaen University.

Reference

- (1) Tritt TM and Subramanian MA. Thermoelectric materials, phenomena, and applications: A bird's eye view. *MRS Bull.* 2006;31(3): 188-194.
- (2) Koumoto K, Terasaki I, and Funahashi R. Complex oxide materials for potential thermoelectric applications. *MRS Bull.* 2006;31(3): 206-210.
- (3) Shikano M and Funahashi R. Electrical and thermal properties of single-crystalline $(\text{Ca}_2\text{CoO}_3)(0.7)\text{CoO}_2$ with a $\text{Ca}_3\text{Co}_4\text{O}_9$ structure. *Appl. Phys. Lett.* 2003;82(12): 1851-1853.
- (4) Fergus JW. Oxide materials for high temperature thermoelectric energy conversion. *J. Eur. Ceram. Soc.* 2012;32: 525-540.
- (5) Daengsakul S, Mongkolkachit C, Thomas C, Siri S, Thomas I, Amornkitbamrung V, et al. A simple thermal decomposition synthesis, magnetic properties, and cytotoxicity of $\text{La}_{0.7}\text{Sr}_{0.3}\text{MnO}_3$ nanoparticles. *Appl. Phys. A.* 2009;96(3): 691-699.
- (6) Daengsakul S, Thomas C, Thomas I, Mongkolkachit C, Siri S, Amornkitbamrung V, et al. Magnetic and Cytotoxicity Properties of $\text{La}_{1-x}\text{Sr}_x\text{MnO}_3$ ($0 < x < 0.5$) Nanoparticles Prepared by a Simple Thermal Hydro-Decomposition. *Nanoscale Research Letters.* 2009;4(8): 839-845.
- (7) Buch JJU, Pathak TK, Lakhani VK, Vasoya NH, and Modi KB. High temperature thermoelectric power study on calcium substituted lanthanum manganites. *J. Phys. D: Appl. Phys.* 2007;40(17): 5306-5312.
- (8) Ang R, Sun YP, Zhu XB, and Song WH. Influence of Te doping on the perovskite manganite $\text{La}_0.5\text{Ca}_0.5\text{MnO}_3$. *Solid State Commun.* 2006;138(10-11): 505-510.
- (9) Ang R, Sun YP, Zheng GH, and Song WH. The magnetothermoelectric power in the Y- and Ho-doped $\text{La}_{0.9}\text{Te}_{0.1}\text{MnO}_3$. *Solid State Commun.* 2008;145(7-8): 337-340.
- (10) Daengsakul S, Mongkolkachit C, Thomas C, Thomas I, Siri S, Amornkitbamrung V, et al. Synthesis and characterization of $\text{LaMnO}_3+\delta$ nanoparticles prepared by a simple thermal hydro-decomposition method. *Optoelec. Adv. Mater. Rapid Commun.* 2009;3(2): 106-109.